

International Journal of Modern Physics B
 © World Scientific Publishing Company

Circuit type simulations of magneto-transport in the quantum Hall effect regime

J. Oswald

Institute of Physics, University of Leoben, Address
 A-8700 Leoben, Austria
 josef.oswald@unileoben.ac.at

Received Day Month Year
 Revised Day Month Year

A Landauer-Büttiker type representation of bulk current transport is used for the numerical simulation of the magneto-transport of 2-dimensional electron systems. It allows us to build up a network model, which describes the effect of non-equilibrium currents injected via metallic contacts like in real experiments. Our model suggests a peak-like contribution of de-localized states to the bulk conductance, which appears embedded in the density of states (DOS) of the Landau levels (LLs). In contrast, the localization picture of the quantum Hall effect suggests almost sharp boundaries between localized and de-localized states and does not explicitly map out their contribution to the bulk conductance. Most recent experiments by B.A. Piot et al. suggest a similar peak-like contribution of de-localized states near the center of the LLs. Our simulation results for the same parameter values as determined by Piot et al reproduce their experimental data very well.

Keywords: quantum Hall effect; network model; enhanced g-factor.

1. Modeling of magneto-transport

Although the basic layout of our network looks similar to the well known Chalker-Coddington (CC) network¹, our handling of the nodes as well as the association of the channels with currents and potentials is substantially different and has nothing to do with the CC model. In the following, only the main facts are summarized and for further details please refer to the cited literature². Fig.1a shows a single node of our network, which transmits potentials from the incoming to the outgoing directed channels, while Fig.1b demonstrates, how a network can be composed by combining several nodes. The transmitted potentials are calculated as follows^{2,3}: $u_2 = (u_1 + P \cdot u_3)/(1 + P)$, $u_4 = (u_3 + P \cdot u_1)/(1 + P)$. The geometry of the sample is defined by shaping the lateral density profile of the carriers, which are distributed over the network grid. The local carriers density enters the nodes via the function P , which depends locally on $E_F - E_{LL}$, with E_F the Fermi energy and E_{LL} the Landau level (LL) center. Therefore P is in general different for different nodes and each involved Landau band is represented by a complete network³. In

2 J. Oswald

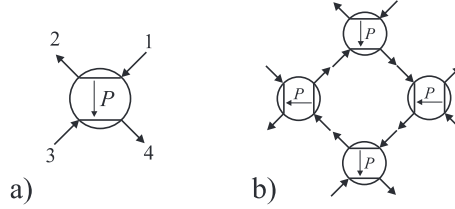


Fig. 1. a) Node of the network with two incoming and two outgoing directed channels. The channels $1 \rightarrow 2$ and $3 \rightarrow 4$ are treated like edge channels with backscattering, where $P = R \square T$ according to the Landauer-Büttiker formalism with R the reflection and T the transmission coefficient. b) Arrangement of the nodes for building the minimal physical element of a network, which is the closed loop of a so called magnetic bound state. The complete network is composed by putting together a sufficient number of such adjacent loops.

this way contact leads, gate electrodes and the effect of inhomogeneities can be modeled. The theoretical basis of P is transmission across saddle points of long range potential fluctuations in the bulk².

$$P = \exp \left[- \frac{L^2 (E_F - E_{LL}) eB}{e\tilde{V} h} \right] \quad (1)$$

The saddle energy corresponds to the LL center E_{LL} , eB/h is the number of states of a LL, L and \tilde{V} are connected to the Taylor expansion of the involved saddle point: L is the period and \tilde{V} the amplitude of a two-dimensional Cosine-potential, which has the same 2nd order Taylor expansion like the actual saddle potential. Representing the encircled saddle in Fig. 2 by an appropriate 2-dimensional Cosine

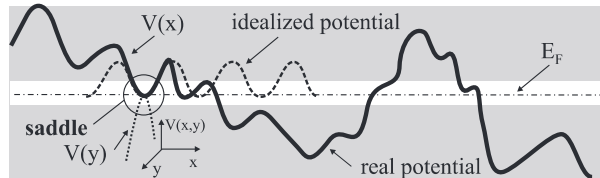


Fig. 2. Schematic one-dimensional representation (x -profile) of a fluctuating potential together with the idealized 2D-Cosine potential with the right Taylor coefficients for representing the encircled saddle.

potential, which matches the saddle curvature, we get the dashed plotted Cosine function. However, the real potential modulation results from a random potential. It is easily seen, that therefore the overall LL broadening Γ will be larger than \tilde{V} .

For the numerical calculation we have two options: (i) we introduce a realistic fluctuating potential modulation, which can be discretized on our periodic network grid (as described in Ref. ²) or (ii) we use a periodic grid of reduced lateral resolution without explicitly including potential fluctuations. For realistically shaped macroscopic sample structures the requirements for option (i) are presently beyond our numerical capabilities and therefore we use the latter one. In case (ii)

L corresponds to a much larger length than the real mean fluctuation period and therefore also the corresponding potential modulation \tilde{V} appears much larger than the real mean fluctuation amplitude. Consequently, neither L nor \tilde{V} have a physical meaning independently from each other. Only the pre-factor of $(E_F - E_{LL})$ in the exponent of Eqn.1 as a whole is relevant. It defines an energy interval for the Fermi level, in which bulk conduction is possible. The overall LL broadening, which we assume to be Gaussian, in this case is only used for calculating the magnetic field dependent Fermi level E_F . Therefore different parameters have to be used for describing $DOS(E_F)$ and the bulk conductance $G_{xx}(E_F)$. This is demonstrated for the most simple case of representing the whole sample by a single node and deriving $G_{xx}(E_F)$ for a single LL⁴: Since $R_{xx} = P \cdot h/e^2$ and $G_{xx} = R_{xx} / (R_{xx}^2 + R_{xy}^2)$, we get $G_{xx} = (e^2/h) \cdot P / (1 + P^2)$, which forms a peak while $P = 0 \rightarrow \infty$. If we plot now $DOS(E_F)$ and $G_{xx}(E_F)$ normalized to each other within the same diagram, we get a situation like shown in Fig.3. While the localization picture maps out localized and

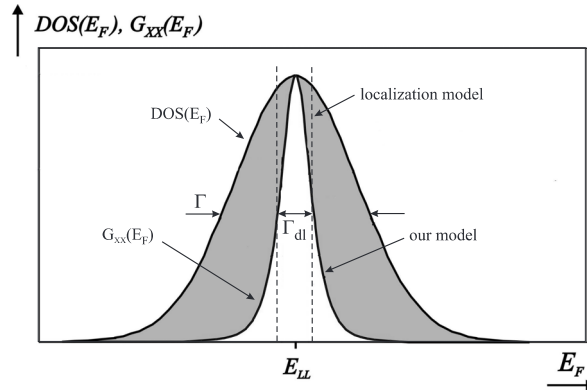


Fig. 3. DOS and conductance G_{xx} versus Fermi energy. Our model suggests a smooth change of the bulk conductance at the boundaries between localized and de-localized states mapped out by the localization model (indicated by the two vertical dashed lines). The light colored G_{xx} -peak can be understood to correspond with the light colored region around the saddle energy in Fig.2. The labeling Γ_{dl} for the conductance peak width has been chosen in accordance to Piot et al as discussed in section 2

de-localized states as a function of energy⁵, our model considers current transport across localized magnetic bound states by tunneling. The associated conductance decays exponentially as a function of the energy like indicated in Fig.3. Such a smearing-out of the sharp boundaries between localized and de-localized states in the observed conductance variation is evident from actual experimental results⁶.

2. Results and conclusion

Our simulations follow most recent experiments by B.A. Piot et al⁶. The authors analyzed experimental data in order to extract the filling factor dependent exchange

4 J. Oswald

enhanced effective g-factor g_{eff} . For the data analysis they assumed the magnetic field dependent longitudinal resistance to be an appropriate tool to monitor directly the DOS at the Fermi level. This led them to assume a peak-like density of current carrying states of width Γ_{dl} (corresponding to the width of our G_{xx} -peak in Fig.3), which appears embedded in the overall DOS of substantially larger width Γ . In order to demonstrate the correspondence with our model, we use the fit parameters of Piot et al as an input and simulate their experimental data. It is important to note, that for our numerical model we have to use a function g_{eff} versus B , which is sample specific, because the physical background is a filling factor dependence of g_{eff} . Furthermore, g_{eff} is only known and extracted at the field positions of appearing spin-splitting in R_{xx} . At magnetic fields away from the observed spin splitting the g-value has no significance for the transport data. Therefore a simple monotonous function has been used for the simulations, which seems to allow a good agreement with the experimental results. Since an overall oscillatory behavior of g_{eff} versus B has to be expected, the used monotonous function for connecting the extracted g-values must not be taken for real. The still achieved very good agreement between simulation and experiment in Fig.4 therefore demonstrates, that transport is not sensitive to spin splitting at arbitrary magnetic fields. The amplitude of the

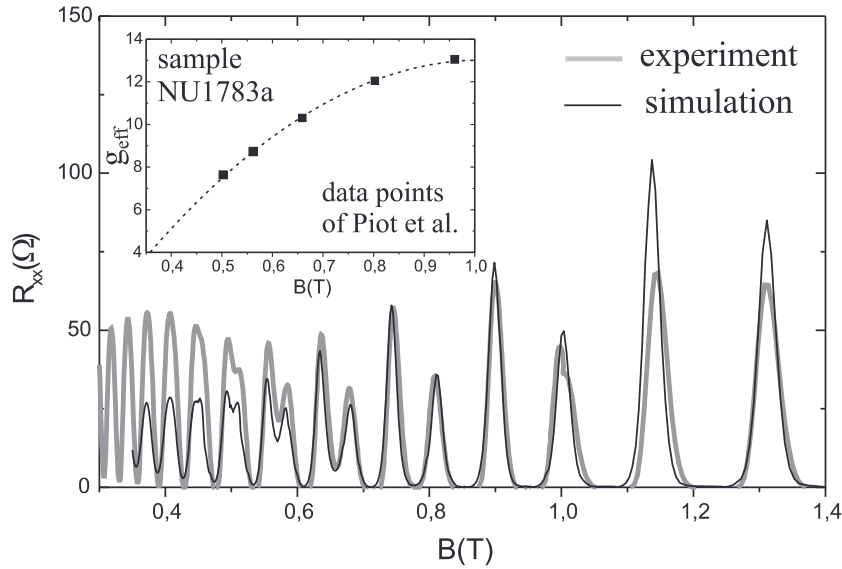


Fig. 4. Simulation results and experimental R_{xx} -data of Piot et al. Simulation parameters: $\Gamma = 6\text{K}$, $\Gamma_{\text{dl}} = 1.48\text{K}$, $n = 2.07 \cdot 10^{11} \text{cm}^{-2}$. The used network consisted of 155×93 nodes. Insert: The dots represent the g-values of Piot et al at the B-field positions of occurring spin splitting. The continuous dotted line is a polynomial fit of g_{eff} versus B . The amplitude of the simulation data is normalized to the amplitude of the experimental data at $B = 0.8$ Tesla.

simulation data in the range above 0.6 Tesla is about a factor of 3 larger than in the

experiment. The additionally obtained Hall resistance R_{xy} provides no additional information and is not shown. Our model addresses also edge-bulk equilibration, which has an influence on the R_{xx} -peak heights⁷. If bulk and the inner edge channel belong to the same LL, we expect a stronger equilibration (increase of the R_{xx} -peak height) as if they belong to different LLs (decrease of the R_{xx} -peak height). In this way the sequence of the alternating peak heights of the spin split LLs is captured correctly by our simulations. The mismatch of the absolute amplitude between simulations and experiments may result from an insufficient representation of the sample geometry and an insufficient representation of the sample edge and thus, missing further details of edge-bulk equilibration. We use the same parameter values as obtained by Piot et al (given in caption of Fig.4) with one exception: For the overall LL broadening Γ we use 6 K instead of 2.2K. Once more it should be pointed out, that for the actual calculation, which does not resolve the native potential fluctuations on the network grid, the individual values for L and \tilde{V} have no physical meaning. Instead, the energy interval defined by the whole pre-factor of $(E_F - E_{LL})$ in the exponent of Eqn.1 is the decisive parameter, which corresponds to Γ_{dl} defined by Piot et al. For the simulation, the expression $(e\tilde{V} \square L^2)(h \square eB)$ has been threaded as a single B-dependent parameter, that was set to match the value Γ_{dl} of Piot et al at $B=0.8T$.

In conclusion we have shown, that by using a circuit type network model for magneto-transport, the main experimental features of R_{xx} can be captured, including the set-in of spin splitting and the corresponding relation of the peak heights. We find a good agreement with an analysis of experimental data by Piot et al, who assume R_{xx} to monitor the density of current carrying states at the Fermi level. They extracted a peak-like distribution of width Γ_{dl} , which appears embedded in the overall DOS of width $\Gamma > \Gamma_{dl}$. Our model indicates a peak-like variation of the bulk conductance, which leads to a very good reproduction of the experimental data for the same parameter values as obtained by Piot et al. Thus, on the one hand, our model confirms the correctness of the data analysis by Piot et al, and in this context it supports to some extent also the idea of a peak-like distribution of de-localized states. On the other hand, however, the only DOS which enters our model is the total DOS of the LLs of width Γ . The embedded conductance peak is a result of our model and therefore a further step towards an interpretation in terms of a density of de-localized states on the background of our model is in principle not compelling.

1. J.T.Chalker, P.D.Coddington, J.Phys. C 21, 2665 (1988)
2. J.Oswald, M. Oswald, J. Phys.: Condens. Matter 18, R101(2006)
3. J. Oswald, A. Homer, Physica E 11, 310 (2001)
4. J. Oswald, G. Span, F. Kuchar, Phys. Rev. B 58 (1998) 15401
5. B. Huckestein, Rev. Mod. Phys. 67, 357 (1995)
6. B.A Piot et al, Phys. Rev. B 72, 245325 (2005)
7. J.Oswald, 15th Int. Conf. on High Magnetic Fields in Semiconductor Physics, SEMIMAG 15, 5-9 Aug, 2002, Oxford, U.K., CD-ROM

